How Much Predictive Skill Is Contained in the Thermal Structure of an Oceanic GCM?

MOJIB LATIF

Max-Planck-Institut für Meteorologie, Hamburg, Federal Republic of Germany

NICHOLAS E. GRAHAM

Scripps Institution of Oceanography, La Jolla, California

19 March 1991 and 6 November 1991

ABSTRACT

The time history of upper-ocean temperatures in the tropical Pacific has been used as a predictor in a statistical prediction scheme to forecast SST anomalies in this region. The temperature variations were taken from the output of an oceanic general circulation model that was forced by observed winds for the period 1961 to 1985. Since such model data are presently used as initial conditions in prediction experiments with coupled ocean–atmosphere models, it is of particular interest to investigate up to what lead time tropical Pacific SST is predictable without the coupling of an atmosphere model to the ocean model.

We compared our results with those obtained by the persistence forecast and with those obtained by using the wind stresses themselves as predictors in a statistical forecast model. It is shown that using the upper ocean temperatures from the ocean model forced by observed winds gives significantly better skills at lead times of 6 to 12 months compared to persistence and to the pure wind-stress model. Off-equatorial heat content anomalies at 5°N are shown to contribute significantly to the predictability at these lead times, while those at 12°N do not.

1. Introduction

Present predictions of the El Niño/Southern Oscillation (ENSO) phenomenon with physical models are conducted in such a way that an ocean model is forced by observed winds up to a certain time when the prediction starts. The ocean fields at this time serve then as initial conditions for the prediction of the future state of ENSO. Thereafter, different assumptions are made on the atmospheric feedback. In the model of Inoue and O'Brien (1984) the winds are held constant at their initial values throughout the forecast period. Cane et al. (1986) couple a simple physical atmosphere model to the ocean, while Latif and Flügel (1991) represent the atmosphere as a linear local feedback. Common to all three models is the assumption that the memory of the coupled ocean–atmosphere system is provided by the ocean and that the past wind fields used to precondition the ocean are the only observational data that enter the prediction.

Here we further investigate the initial conditions used in the prediction experiments of Latif and Flügel (1991). We focus on the question of how much predictive skill these initial conditions contain on their own. The background for doing so is that the evidence is growing that ENSO is a cycle and is therefore inherently predictable to some degree. In their paper, Latif and Flügel (1991) describe in more detail such a cycle in their oceanic general circulation model (OGCM) when forced by observed winds. They find one dominant mode of variability showing a slow eastward-propagating signal in subsurface temperatures at the equator with a speed in the western Pacific about one order of magnitude less than the first baroclinic mode Kelvin wave speed. This result is shown to be consistent with the analysis of observed sea levels. A similar result was obtained by Philander (1990) in his investigation of the variability of equatorial upper-ocean heat content simulated by his OGCM in a run with observed winds.

Latif and Flügel (1991) explain their findings with an accumulation of warm water in the equatorial Pacific prior to El Niño events in response to the trade winds and a subsequent heat loss of the equatorial region during the event, as was proposed by Wyrtki (1985). Zebiak and Cane (1987) attributed the oscillatory behavior found in their coupled model integration to essentially the same mechanism. Philander (1990) describes his results as a generalization of the "delayed action oscillator" (Schopf and Suarez 1988; Graham and White 1988), in which a superposition of many wave modes plays an important role in determining the delayed response of the ocean. The net effect of these waves is to modulate the equatorial heat

Corresponding author address: Dr. Mojib Latif, Max-Planck-Institut fur Meteorologie, D-2000, Bundesstr.55, Hamburg 13, Germany.

content and currents, effects that may then be amplified by the atmospheric feedback.

These studies indicate that the tropical Pacific has a relatively long memory to past winds and it is just this memory that provides the physical basis for ENSO prediction. Since the "memory" is associated with thermocline displacements, the state of the ocean with respect to the ENSO cycle could be estimated by continuously monitoring subsurface temperatures in the equatorial Pacific. However, the spatial coverage of such observations is limited so that we have to seek other possibilities until the data situation has considerably improved. One possible way is to make use of ocean models that have been shown to realistically simulate the interannual variability in the tropical Pacific when forced by observed winds (e.g., Busalacchi et al. 1983; Philander and Seigel 1985; Latif 1987).

In this paper we investigate the use of such data from an OGCM forced by observed winds. Our main interest is how much information these data contain with respect to the future development of the real ocean. For this purpose we have used the model temperatures within the upper 300 m as predictors in a statistical prediction scheme for the prediction of observed SST changes (Fig. 1). The results of our study provide not only an estimate of the oceanic memory but also an idea up to which lead time the nonlinear effects inherent in the coupling of the atmosphere and the ocean are of minor importance with respect to the time evolution of equatorial SST anomalies.

Our results suggest that the phase of tropical Pacific SST anomalies is predictable several months in advance using the time history of the model temperatures. The lead time critically depends on the season with significant skills up to as much as 15 months. In contrast, using instead of the model temperatures the wind-stress fields used to drive the ocean model themselves as predictors in the statistical prediction scheme yields significant skills only for lead times of a few months. This indicates that the ocean acts as a complicated space–time filter on the winds.

The paper is organized as follows. In section 2 we describe the ocean model, the prediction scheme, the predictor, and the predictand data. Section 3 deals with the investigation of the space–time structure of the upper-ocean temperatures taken from the run with the ocean model forced by observed winds. In section 4 we present the results of our predictions of tropical Pacific SST using the model temperatures and the winds used to force the ocean model as predictors. The paper ends with a summary and a discussion of the results in section 5.

2. Ocean model, prediction scheme, and data

a. Ocean model

The ocean model described by Latif (1987) is a regional oceanic general circulation model (OGCM) of the tropical Pacific. The meridional resolution is variable, with 50 km near the equator increasing to about 400 km at the northern and southern boundary at ±30°. The grid distance in the zonal direction is constant at 670 km. In the vertical there are 13 levels, with ten of them being placed in the upper 300 m. The ocean model mimics real coastlines but includes no bottom topography. The ocean floor is at a constant depth of 4000 m. Vertical mixing coefficients are Richardson number dependent (Pacanowski and Philander 1981).

The ocean model was spun up with climatological forcing for four years. Thereafter, the observed wind stresses drive the model for the period 1961 to 1985. The surface wind stresses have been taken from the Florida State University (FSU) dataset (Goldenberg and O'Brien 1981; Legler and O'Brien 1984). The performance of the model with respect to the observed SST anomalies is shown in Fig. 2 for the so called "SST-3" region (Graham et al. 1987b), which is an area average over the region 5°N–5°S and 170°W–120°W.

The observed SST anomalies in this region will serve as predictands for the statistical predictions described in section 4. Interannual variability in the SST-3 region is realistically simulated by the ocean model as indicated by the correlation of 0.78. Problems are found during the cold phases, during which the model tends to systematically underestimate the strength of the SST anomalies. The root-mean-square (rms) error is therefore quite large with 0.49°C, which is about two-thirds of the standard deviation of the observed SST anomalies ($\sigma_{obs} = 0.77$°C). Nevertheless, we have some con-

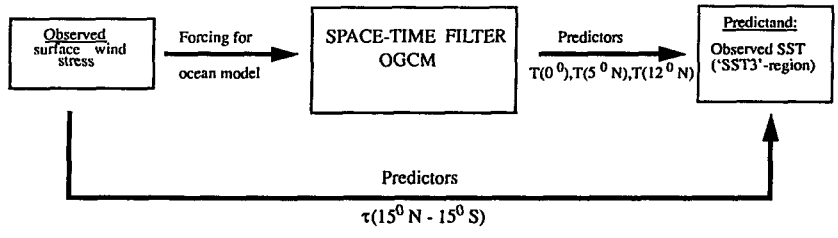

FIG. 1. Schematic diagram of the experimental setup.

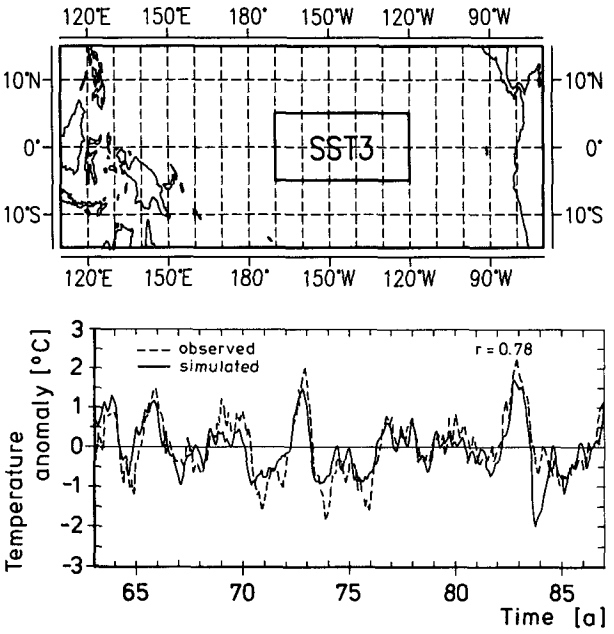

FIG. 2. Upper: SST-3 region over which the results of the prediction experiments have been averaged. Lower: Comparison of observed (dashed) and simulated (solid) SST anomalies averaged over the SST3 region.

fidence in our ocean model to be used in the investigation of the predictability of tropical Pacific SST anomalies.

b. *Prediction scheme*

The statistical prediction scheme is based on the canonical correlation analysis (CCA) technique introduced by Hotelling (1935). Barnett and Preisendorfer

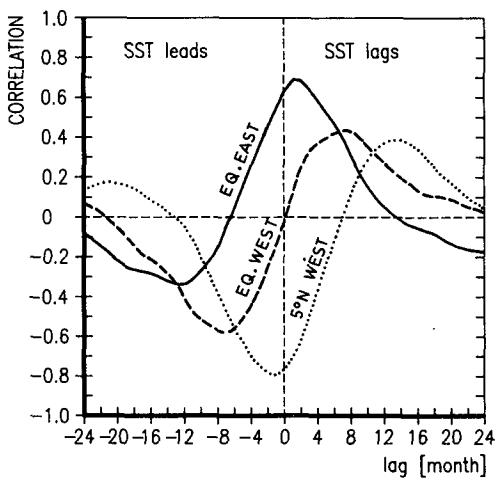

FIG. 3. Lagged cross correlations of SST anomalies in the SST3-region with simulated heat content anomalies in three different regions.

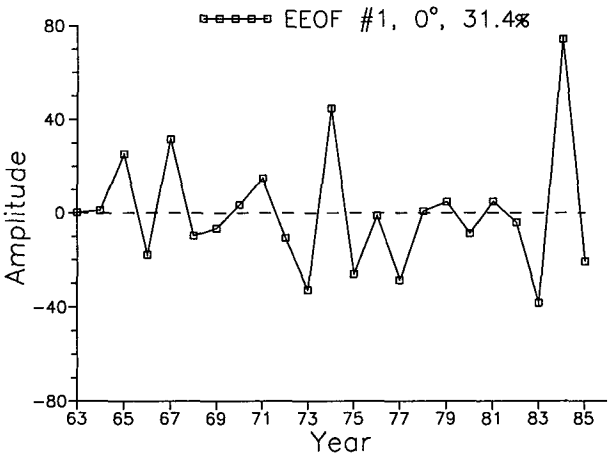

FIG. 4. Time series of the first EEOF of the temperature anomalies simulated along the equator in the upper 300 m.

(1987) used the CCA approach for the prediction of United States air temperature. Graham et al. (1987a,b) used this technique for the prediction of ENSO from surface wind and sea level pressure fields. In both studies the CCA and its use in statistical predictions are described in detail. We followed their procedure precisely and therefore refer to these two papers for further details. As outlined by Graham et al. (1987a), the CCA technique finds linear combinations of two datasets that are most highly correlated. In contrast to EOF analysis, CCA deals with the "between-field" variability rather than with the "in-field" variability, but like empirical orthogonal function (EOF) analysis CCA allows the filtering and depiction of major modes of (co)variability.

As predictors we used the extended empirical orthogonal functions (EEOFs) (e.g., Graham et al. 1987a) of different quantities. In contrast to ordinary EOFs, the EEOFs have the advantage of yielding information about the time evolution of spatial patterns. To compute the EEOFs, the fields are taken at different time lags and data at different locations and different times are treated as independent variables in order to estimate an "extended" covariance matrix. The eigenvectors of this extended covariance matrix are referred to as EEOFs.

Since CCA is a form of linear regression, one has to be cautious in using it in prediction studies, because the hindcast skills might be highly artificial. Following the study of Graham et al. (1987b), we therefore have cross validated our skills, which means that the statistical models have been constructed in such a way that the time period a prediction has been made for was excluded. Although the applied cross-validation technique does not remove the total artificial skill, as discussed by Graham et al. (1987b), our skills are expected to be close to the "true" skill, hereafter referred to as forecast skill.

In order to estimate the seasonal dependence of the forecast skills, CCA has been carried out for different initialization months, namely, January, April, July, and October. A CCA model has therefore been constructed for each initialization month and for each lead time. We used nine lead times, each two months apart from each other, ranging from 1 to 17 months lead.

We used both correlation and rms error as scores, which yield information about the phase and the amplitude, respectively, instead of the traditional skill measure expressed as explained variance, as used in many other studies (e.g., Graham et al. 1987b). However, a rough estimate of the explained variance can be obtained by squaring the correlations.

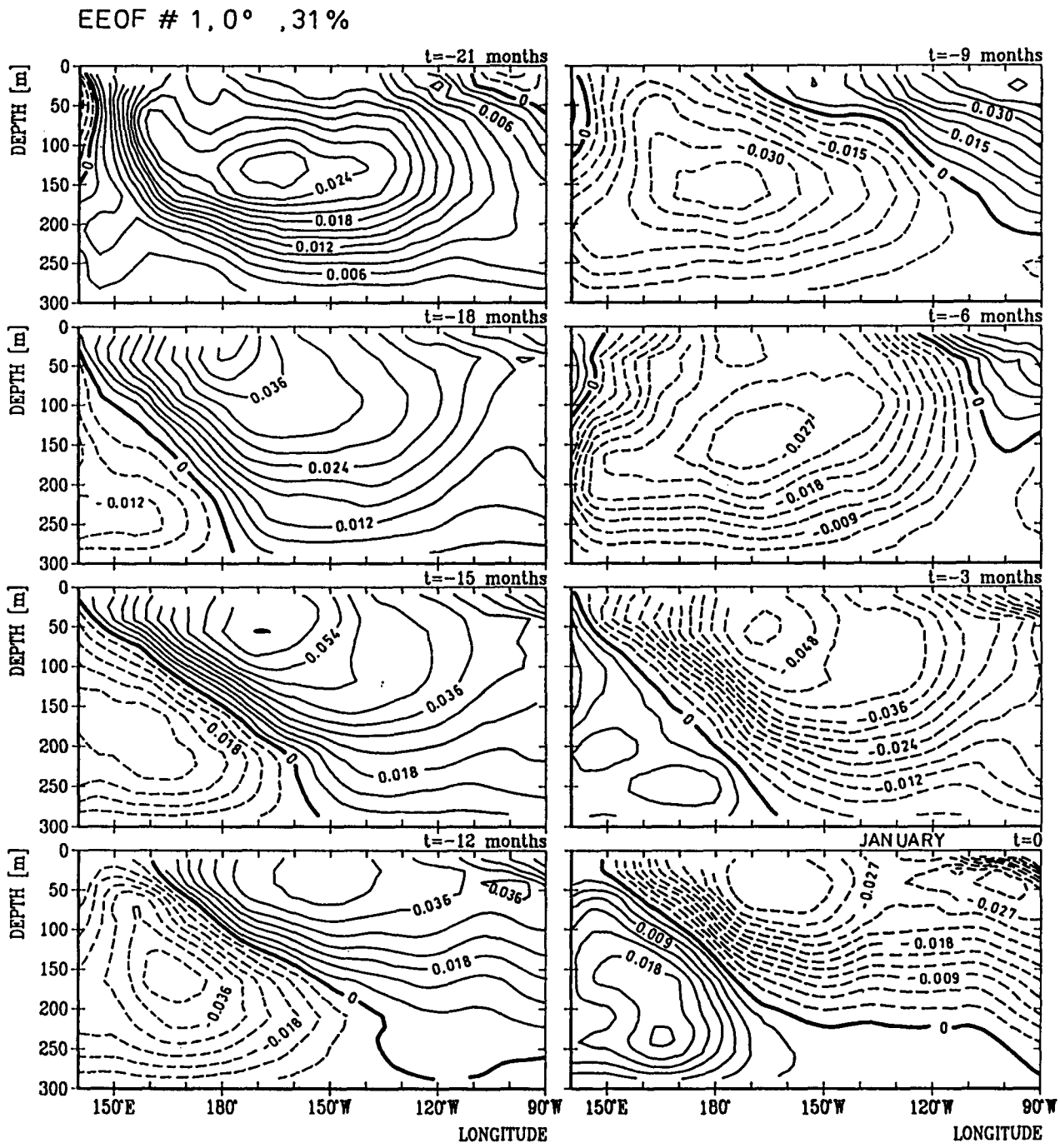

FIG. 5. Spatial patterns for the first equatorial EEOF. Individual maps are three months apart from each other.

c. Predictor and predictand data

We used the first five EEOFs of the following quantities in the CCA analysis:

1) The monthly model temperatures in the upper 300 m along the equator, $T(0°)$ model,
2) the monthly model temperatures in the upper 300 m along 5°N, $T(5°N)$ model,
3) the monthly model temperatures in the upper 300 m along 12°N, $T(12°N)$ model, and
4) the three-month averages of the observed wind stress fields over the tropical Pacific from 15°N to 15°S used to drive the ocean model.

The first five EEOFs pick up typically between 70% and 80% of the total variance in the temperature data and typically 40% to 50% in the wind-stress data. The EEOFs use information at eight time lags each three months apart from each other, so that the time history of the past 21 months is used for the predictions. For use as predictors in the prediction scheme, the stress data were smoothed onto a 10° × 4° (longitude × latitude) grid. In order to remove the high-frequency noise in the stress data, 3-month averages have been used in the predictions instead of monthly values as for the model temperatures. (We note that we did not use monthly mean values for the model temperatures, but rather instantaneous values simulated at the end of each calendar month. This can be justified because of the high persistence of ocean temperatures.)

As predictands, we used the first five ordinary EOFs of the observed SST anomalies for the particular month predictions are made for. The SST data (see Graham and White 1990) are comprised of a combination of Comprehensive Ocean Atmosphere Data Set (COADS) and Climate Analysis Center (CAC) analyses. Finally, the results of the predictions have been averaged onto the SST-3 region (Fig. 2) for which the comparisons with the observed SST changes have been made.

3. Heat content variations and predictor field characteristics

Motivation for the present study can be obtained from a simple correlation analysis of model heat content anomalies with observed SST changes in the SST-3 region (Fig. 3). The heat content is defined here as the integral over the temperatures from the surface to 225 m. We used heat content anomalies averaged over three different key regions for our correlation analysis: 1) The equatorial east Pacific (0°, 152°W–85°W), 2) the equatorial west Pacific (0°, 142°E–158°W), and 3) the northern west Pacific (5°N, 142°E–158°W).

The most important feature in Fig. 3 is the shift of the maximum in the correlation function to larger lags. This behavior suggests a propagation of information from the western Pacific off the equator into the equatorial waveguide, in which the signal propagates eastward. Since the speed of this propagation, as indicated by the correlation structure, is much slower than expected from the gravest equatorial wave modes, either a superposition of many different wave modes or advective processes must be important.

We then analyzed by means of EEOF analysis the model temperature anomalies in the upper 300 m at the equator and at 5°N to investigate the variability patterns that accompany the heat content variations. As described in section 2c, the EEOFs were calculated using eight time lags each 3 months apart. Thus, each EEOF represents a pattern of evolution of upper ocean temperatures over a period of 21 months. Here we present the analyses for the evolution of temperature anomalies simulated by the ocean model in January, when SST anomalies at the equator are in general well developed.

The leading EEOF of the temperature anomalies along the equator accounting for 31% of the total variance appears to be associated with the ENSO phenomenon. Its coefficient time series (Fig. 4) shows, for instance, indications of the two major warm events of 1972–73 and 1982–83, as well of the observed cold events during the analyzed period. However, while the phase compares quite nicely with indices of ENSO, the amplitude does not (e.g., Fig. 2). The extraordinary cold event of 1984 is related to the fact that the wind stresses used to force the ocean model, the so-called FSU winds (Goldenberg and O'Brien 1981), exhibit at and near the equator the strongest easterly stress anomalies during the whole 25-year record at the end of 1983 (e.g., Latif 1987, his Fig. 11).

The corresponding evolution of the spatial patterns (Fig. 5) given by the first EEOF shows a regular eastward propagation of temperature anomalies along the equator. Strong evidence is found that the anomalies emanate from the western boundary, which can be seen

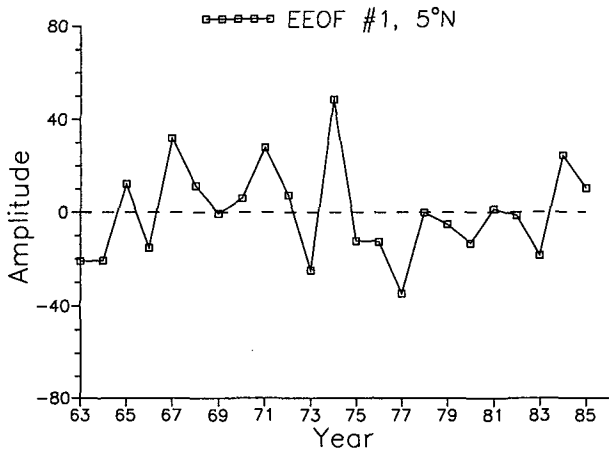

FIG. 6. Time series of the first EEOF for the temperature anomalies simulated along 5°N in the upper 300 m.

by following the negative SST anomalies simulated at time zero backward in time. The negative anomaly can clearly be traced back to the western equatorial Pacific to lag −18 months, which corresponds to the warm phase of the simulated ENSO. At this time the negative anomaly is centered near the western boundary at subsurface levels near 250 m, which is consistent with the "delayed action oscillator" theory (Schopf and Suarez 1988). It then propagates eastward well below the surface until it is able to affect the SST in the central Pacific at lag −9 months. Thereafter, the eastward propagation can also be seen at the sea surface and coupled processes such as those described by Zebiak and Cane (1987), Schopf and Suarez (1988), Battisti (1988), Neelin (1991), and Barnett et al. (1991) may become important. At lag −0, during the well-devel-

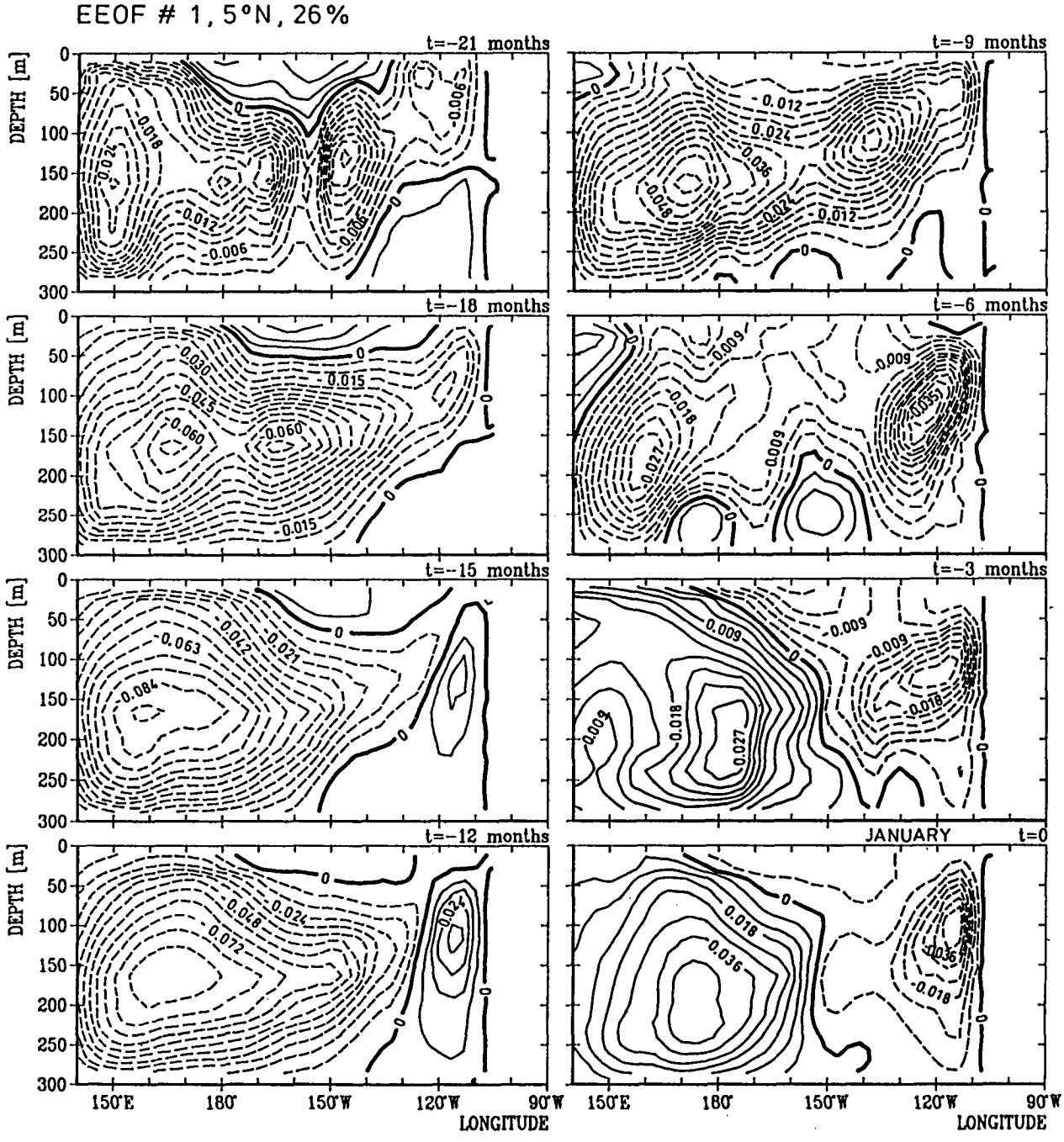

FIG. 7. Spatial patterns for the first EEOF at 5°N. Individual maps are three months apart from each other.

oped cold phase (SST anomalies are mostly negative along the equator), the beginning of the phase reversal is evident at subsurface levels.

The leading EEOF at 5°N, accounting for about 26% of the total variance, is shown in Figs. 6 and 7. Its coefficient time series (Fig. 6) is highly correlated ($r = 0.75$) with the coefficient time series of the leading EEOF at the equator (Fig. 4) so that the EEOF patterns at 5°N can be discussed in conjunction with that at the equator (Fig. 5). At time zero, when SST anomalies at the equator are strongly negative, a well-developed positive anomaly can be seen at 5°N centered near the date line at about 200-m depth. It is likely that this off-equatorial positive subsurface temperature anomaly is generated by Ekman pumping in response to the strong meridional shear of the easterly wind stress anomalies observed during the cold extreme of ENSO, as suggested by Graham and White (1988) and Philander (1990). The positive anomaly can be traced back in time only up to lag −3 months, because no significant SST anomalies that could affect the atmosphere are found at the equator prior to this time. A similar behavior is found during the warm phase of ENSO at lag −18 months, during which a strong negative subsurface temperature anomaly at 5°N is generated.

There does not appear to be evidence of westward phase propagation at 5°N, as suggested by the delayed action oscillator hypothesis (Schopf and Suarez 1988). Instead, the anomalies tend to develop in place and they exhibit considerable strength only during periods of well-developed SST anomalies at the equator. A further inspection of heat content anomalies (not shown) showed that westward propagation occurred at 5°N during particular time periods. This westward propagation was most pronounced prior to the 1972–73 ENSO event, in 1970 and 1971. However, during other periods the heat content anomalies were indeed dominated by a standing component or even showed eastward propagation, as during the huge warm event of 1982–83.

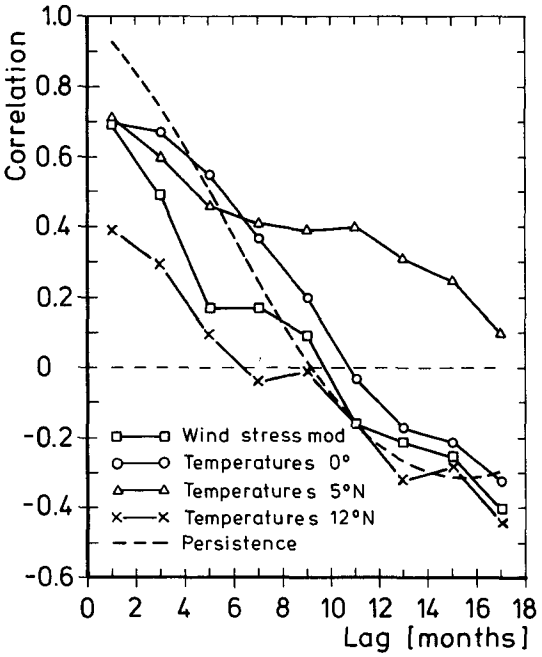

FIG. 8. Cross-validated anomaly correlation coefficients for the different forecast models.

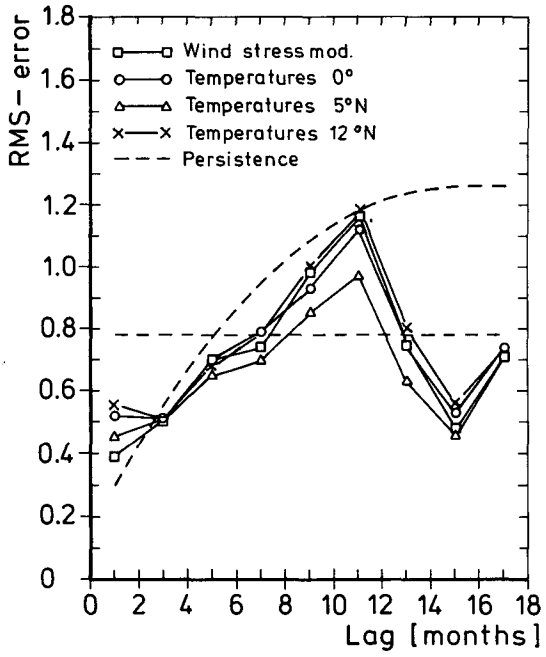

FIG. 9. Rms errors (°C) for the different forecast models. The horizontal dashed line shows the standard deviation σ_{obs} of the observed SST-3 anomalies.

4. Prediction experiments

We have shown that SST anomalies in the eastern equatorial Pacific appear to be preceded by a characteristic evolution of equatorial and off-equatorial heat content anomalies. Although, as previously indicated, much variance remains unexplained by the described evolution in heat content, our findings show that this evolutionary pattern can be exploited to predict the future state of ENSO. To estimate up to what lead times this might be possible, we used the time history of the upper-ocean temperatures derived from our ocean model as predictors in a statistical prediction scheme to forecast the observed changes in equatorial Pacific SST.

a. Skills

Figure 8 shows the cross-validated anomaly correlation coefficients for the different forecast models, namely, for the temperature models using data from

TABLE 1. Cross-validated correlations for the T(0°) model.

	Feb	Apr	Jun	Aug	Oct	Dec	Feb	Apr	Jun
From Jan:	0.7	0.4	−0.2	−0.3	0.1	0.1	0.2	0.2	−0.5
	May	Jul	Sep	Nov	Jan	Mar	May	July	Sep
From Apr:	0.4	0.5	0.6	0.5	0.4	0.4	−0.3	−0.6	−0.5
	Aug	Oct	Dec	Feb	Apr	Jun	Aug	Oct	Dec
From Jul:	0.7	0.7	0.7	0.7	0.1	−0.7	−0.7	−0.4	−0.3
	Nov	Jan	Mar	May	Jul	Sep	Nov	Jan	Mar
From Oct:	0.8	0.8	0.6	−0.2	−0.4	−0.2	−0.2	−0.2	−0.1

0°, 5°N, and 12°N, and for the wind-stress model. For reference the persistence forecast is shown as well. At short lead times all models, except the one using the model temperatures at 12°N, give reliable forecast skills with cross-validated correlations on the order of 0.7 for the one-month predictions. However, significantly better correlations than those derived from the persistence forecast are obtained only from the temperature models. Using the model temperatures at the equator gives better correlations beginning with forecast lags of 5 months. However, the evolution of the correlation closely follows that of the persistence forecast, exhibiting a rather rapid drop in the anomaly correlation at longer lead times.

The most striking feature in Fig. 8 and a major finding from this work is that the use of temperatures simulated at 5°N significantly improves the predictions at lead times larger than 5 months. This result clearly suggests the importance of off-equatorial heat content anomalies for the future development of eastern equatorial SST. The evolution of the anomaly correlation shows a constant correlation up to forecast lags of 11 months. Further, the difference in the shapes of the curves is striking.

Although the cross-validated correlations are low at about 0.4, they are statistically significant at the 95% significance level. In assessing the statistical significance of correlations, one has to estimate the number of degrees of freedom. This number is not simply given by the number of forecasts, because individual forecasts are not independent from each other. A measure of the effective time between independent samples can be estimated by the autoregressive properties of both time series [Livezey and Chen (1983), their Eq. (1)]. The decorrelation time is at the order of 9 months, which gives about 30 degrees of freedom. This requires a correlation of 0.33 to be exceeded for the 95% significance level in a t test.

The level of the correlation can probably be increased by making use of all information available from the ocean model, instead of using information from one latitude only or by making use of observational data from subsurface levels. Also, seasonal SST forecasts may have higher skills, because monthly SST data still contain considerable high-frequency noise. Further, if statistical predictions were made for the SST anomalies derived from the uncoupled ocean model run with observed winds, the correlation at a lead time of 11 months amounts to about 0.6 (not shown). This demonstrates that eastern Pacific SST is potentially predictable at lead times of about one year from subsurface data only.

Comparing the correlations obtained with the T(0°) model and the T(5°N) model to those obtained with the wind-stress model, it becomes obvious that by running the wind stresses through an ocean model and making use of the model data, rather than of the wind stresses themselves, considerably increases the forecast skill. The wind-stress model yields even smaller correlations than those obtained by the persistence forecast. At small lead times the correlations from the wind stress model are also lower compared to those obtained by Graham et al. (1987b), who used the surface winds as predictors. One possible reason for this discrepancy might be the fact that Graham et al. (1987b) used monthly values instead of 3-month averages, as in our

TABLE 2. Cross-validated correlations for the T(5°N) model.

	Feb	Apr	Jun	Aug	Oct	Dec	Feb	Apr	Jun
From Jan:	0.8	0.4	0.2	0.2	0.4	0.4	0.5	0.5	−0.2
	May	Jul	Sep	Nov	Jan	Mar	May	Jul	Sep
From Apr:	0.3	0.1	0.4	0.4	0.5	0.4	0.3	−0.4	−0.4
	Aug	Oct	Dec	Feb	Apr	Jun	Aug	Oct	Dec
From Jul:	0.6	0.6	0.6	0.6	0.4	0.3	0.1	0.2	0.3
	Nov	Jan	Mar	May	Jul	Sep	Nov	Jan	Mar
From Oct:	0.8	0.8	0.5	0.3	0.1	0.4	0.3	0.3	0.2

TABLE 3. Cross-validated correlations for the wind-stress model.

	Feb	Apr	Jun	Aug	Oct	Dec	Feb	Apr	Jun
From Jan:	0.9	0.3	−0.4	−0.1	−0.3	−0.2	0.0	0.4	−0.4
	May	Jul	Sep	Nov	Jan	Mar	May	Jul	Sep
From Apr:	0.2	−0.1	−0.2	0.1	0.2	0.3	0.1	−0.3	−0.4
	Aug	Oct	Dec	Feb	Apr	Jun	Aug	Oct	Dec
From Jul:	0.4	0.2	0.2	0.4	0.5	−0.2	−0.5	−0.6	−0.5
	Nov	Jan	Mar	May	Jul	Sep	Nov	Jan	Mar
From Oct:	0.8	0.8	0.7	0.2	−0.5	−0.5	−0.4	−0.4	−0.2

case. Nevertheless, our results imply that the ocean acts as a complicated space–time filter on the winds.

Using the model temperatures at 12°N apparently does not significantly contribute to the predictability at any lead time. This result may be model dependent and is in contrast to conceptual and observational studies (e.g., Pazan et al. 1986, Graham and White 1988) in which it was suggested that considerable information with respect to the ENSO cycle may be contained at latitudes well away from the equatorial strip. On the other hand, Battisti (1988), who investigated the interannual variability simulated by a coupled ocean–atmosphere model, emphasizes the dominant role of the near-equatorial region (5°N–5°S) for the low-frequency behavior of the coupled model, which is consistent with our findings.

The cross-validated rms errors (Fig. 9) were calculated by removing the means prior to the analysis so that the systematic bias has been removed. None of the applied models is able to predict the amplitude changes in equatorial SST anomalies. Although all models yield errors smaller than the persistence errors, the errors are quite large even at short lead times. After about 7 months the errors exceed the standard deviation of the observed SST anomalies. However, also with respect to the rms error the T(5°N) model gives generally better results compared to the other models. All rms errors show a distinct minimum at lead times of 15 months. The reason for this behavior is not yet clear, but it is interesting that Graham et al. (1987b) also found low but significant skill at this lead time for their statistical model based on the evolution of sea level pressure patterns.

In summary, our results indicate that the phase of eastern equatorial SST anomalies is predictable several months in advance from subsurface ocean model data without making use of any ocean observations and neglecting any atmospheric feedback. Further, the lag dependence of our correlations shows an obvious similarity to that obtained by Goswami and Shukla (1991), who used the coupled model developed by Zebiak and Cane (1987) to predict SST anomalies in the eastern equatorial Pacific. Goswami and Shukla (1991) found a similar plateau in the anomaly correlation at lead times of about 6 to 12 months.

b. Seasonal dependence

The cross-validated anomaly correlations derived from the two temperature models using data at the equator and at 5°N and from the wind-stress model are shown in Tables 1, 2, and 3 as function of the month of initialization and of the lead time. All three models show a tendency to perform best during winter and worst during spring. This result is consistent with other ENSO prediction studies (Graham et al. 1987b; Goswami and Shukla 1991; Latif and Flügel 1991). This behavior becomes even more pronounced when analyzing the corresponding hindcast skills. A typical example is given in Fig. 10 showing the hindcast skills for the T(0°) model initialized in four different months. It is apparent that the correlations drop significantly in the spring independent of the initialization month. Evident also is a tendency for the correlations to recover thereafter, which is most pronounced for the predictions initialized in January. Furthermore, the correlations for the predictions started in April are systematically lower than those for the predictions started in the other months. As just described, the hindcast skills are highly artificial because the CCA technique is a least-squares technique. However, it is suggestive

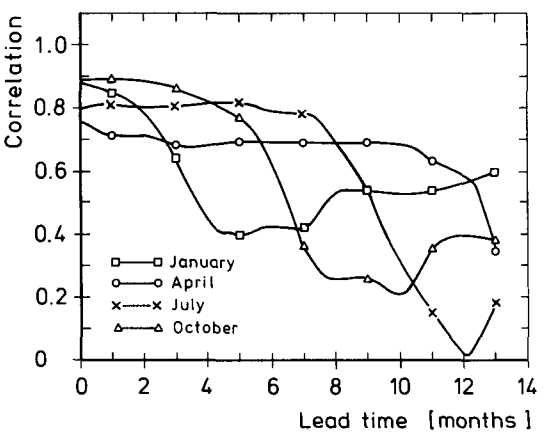

FIG. 10. Hindcast correlation skills as a function of the lead time for the T(0°) model initialized in different months.

that the seasonal dependence of the skills (Fig. 10) shows up so clearly even when the results are not cross validated.

c. *Individual forecasts*

In Fig. 11 we present the individual 5-month lead forecasts from the temperature model that uses the information from the equator. The forecasts in general nicely reproduce the low-frequency changes in the observed SST anomalies. However, the model shows the tendency to predict changes slightly later than observed, which explains the relatively low correlation of $r = 0.55$. The same systematic bias was reported by Graham et al. (1987b), who used surface wind anomalies as predictors. The forecasted amplitudes also show some correspondence to the observed strength of the anomalies, although the rms error is with 0.71°C, rather high compared with the standard deviation of the observed SST anomalies ($\sigma_{obs} = 0.77$°C).

During two periods the model seriously failed. During 1975 the T(0°) model predicted a moderate warming, while the observations show a pronounced cold event. Similar results are reported by Goswami and Shukla (1991), Graham and White (1990), and Xu and Storch (1990). This period is also known as the aborted El Niño. An inspection of the equatorial heat content anomalies (not shown) showed that strong positive anomalies were simulated in the western Pacific by our ocean model prior to the cold event during 1974 (see also Figs. 4 and 6). The T(0°) model also failed to predict the large amplitude during the 1982–83 warm event.

A similar comparison is shown in Fig. 12 for the 11-month lead forecasts obtained from the temperature model that uses only information from 5°N. The correlation skill is 0.40 and the rms error amounts to 0.97°C, which is considerably higher than the standard deviation of the observed SST anomalies. The T(5°N) model also reproduces the basic aspects of the low-frequency variations in the observed SST anomalies, but as indicated by the rather high rms error there appears to be no skill in reproducing the observed strength of the anomalies. Also, the cold event of 1975 and the major warming of 1982–83 are not predicted by the T(5°N) model at this particular lead time.

5. Concluding remarks

We have investigated the surface and subsurface temperatures simulated with an oceanic general circulation model forced by observed winds and have used the time history of the model temperatures as predictors in a statistical prediction scheme to forecast observed SST changes in the tropical Pacific. Our results show that considerable information on the time evolution of the phase of tropical Pacific SST anomalies is contained in such model data. It has been shown that during periods of well-developed SST anomalies in the eastern equatorial Pacific anomalies of opposite sign are excited off the equator at subsurface levels, as expected from linear theory. Consistent with the "delayed action oscillator" concept these signals significantly contribute to the predictability of eastern equatorial SST anomalies at long lead times. Considering the fact that both the wind-stress data used to force the ocean model and the ocean model itself contain serious errors, our results indicate that tropical Pacific SST is predictable about one year in advance from observed subsurface data.

The forecast skills are highly dependent on the season: The SST anomalies in winter are best and those in spring are least predictable. This is in accord with other prediction studies and with the theoretical study of Battisti and Hirst (1989), who showed by analyzing the coupled model of Zebiak and Cane (1987) that the growth of perturbations is large during winter and least during spring.

It has been shown further that forcing an ocean model with observed wind stresses and using the model temperatures instead of the stresses themselves as predictors remarkably increases the skill in predicting the observed SST changes. While the pure wind-stress model generally yields correlations worse than those

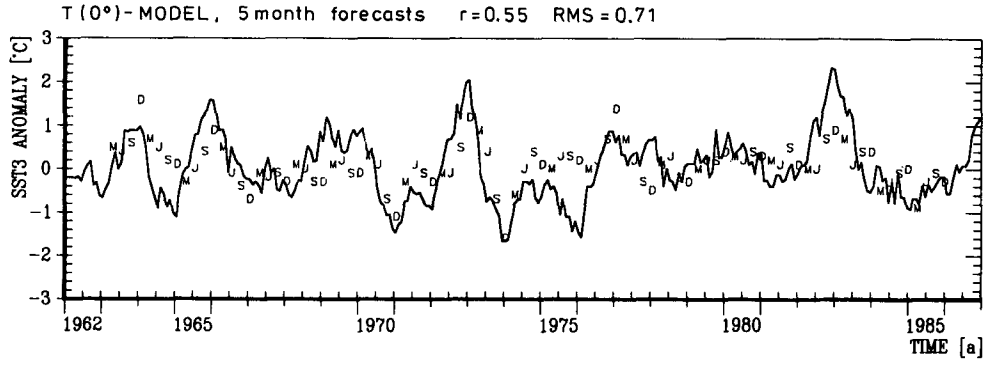

FIG. 11. Individual 5-month forecast for the T(0°) model. The letters indicate the month for which a prediction was made.

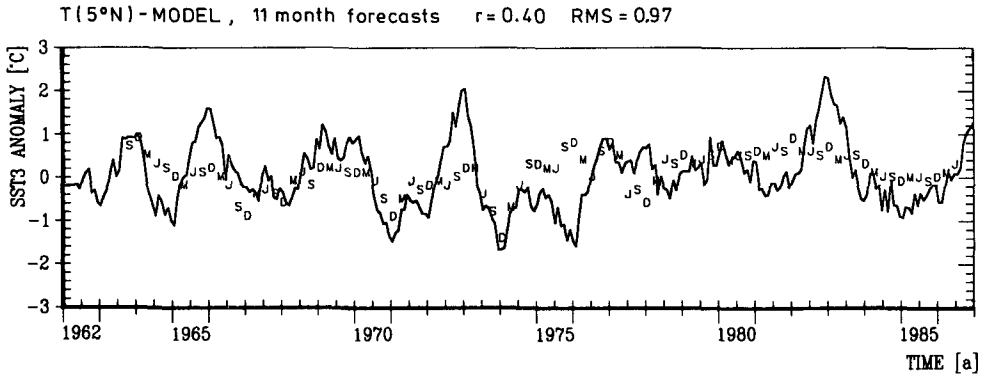

FIG. 12. Individual 11-month forecast for the T(5°N) model. The letters indicate the month for which a prediction was made.

obtained from the persistence forecast, the forecasts based on the model temperatures are in general superior to the persistence forecast at lead times longer than six months.

The lag dependence of the correlations presented here is similar to that shown by Goswami and Shukla (1991) for the coupled model of Zebiak and Cane (1987), although their correlations are slightly higher. We note that Goswami and Shukla (1991) verified against the uncoupled ocean model simulation with observed winds. However, the lag dependence of the correlations, when the results are verified against observations, is very similar (Zebiak, personal communication). Further, they averaged the results over the "Niño 3" region, in contrast to the SST-3 region that we use. However, the differences between these two regions are small. On the other hand, it is interesting that our forecast skills are significantly higher than those presented by Latif and Flügel (1991), who used the same ocean model (coupled to a linear and local atmospheric feedback model). One possible reason for the large difference in skill might be the too diffusive thermocline simulated in the ocean model, a problem also noticed in many other OGCMs. A too diffusive thermocline reduces the sensitivity of SST to thermocline displacements so that an important piece of information might not be communicated from subsurface levels in the western to the sea surface in the eastern Pacific. Therefore, coupled GCMs could successfully be used in ENSO prediction experiments only, if the time-averaged mean state is realistically simulated or prescribed by special correction techniques, such as the flux correction technique (Sausen et al. 1988).

Acknowledgments. The authors would like to thank Dr. Tim Barnett for many fruitful discussions and for making the visit of Mojib Latif to the SCRIPPS Institution of Oceanography possible. We are indebted to Prof. Dr. J. J. O'Brien for providing the surface wind stress dataset. Many thanks also to Mrs. Marion Grunert for preparing the diagrams.

REFERENCES

Barnett, T. P., and R. Preisendorfer, 1987: Origins and levels of monthly forecast skill for United States surface air temperatures determined by canonical correlation analysis. *Mon. Wea. Rev.*, **115**, 1825–1850.

——, M. Latif, E. Kirk, and E. Roeckner, 1991: On ENSO physics. *J. Climate*, **4**, 487–515.

Battisti, D. S., 1988: Dynamics and thermodynamics of a warming event in a coupled tropical atmosphere–ocean model. *J. Atmos. Sci.*, **45**, 2889–2919.

——, and A. C. Hirst, 1989: Interannual variability in a tropical atmosphere-ocean model: Influence of the basic state, ocean geometry and nonlinearity. *J. Atmos. Sci.*, **46**, 1687–1712.

Busalacchi, A. J., K. Takeuchi, and J. J. O'Brien, 1983: Interannual variability of the equatorial Pacific. *Hydrodynamics of the Equatorial Ocean.* J. C. J. Nihoul, Ed., Elsevier Oceanogr. Ser., Vol. 36.

Cane, M. A., S. E. Zebiak, and S. C. Dolan, 1986: Experimental forecasts of El Niño. *Nature*, **321**, 827–832.

Goldenberg, S. O., and J. J. O'Brien, 1981: Time and space variability of tropical Pacific wind stress. *Mon. Wea. Rev.*, **109**, 1190–1207.

Goswami, B. N., and J. Shukla, 1991: Predictability of a coupled ocean–atmosphere model. *J. Climate*, **4**, 3–22.

Graham, N. E., and W. B. White, 1988: The El Niño cycle: A natural oscillator of the Pacific Ocean–Atmosphere system. *Science*, **240**, 1293–1302.

——, and ——, 1990: On the role of the western boundary in the ENSO cycle: Experiments with coupled models. *J. Phys. Oceanogr.*, **20**, 1935–1948.

——, J. Michaelsen, and T. P. Barnett, 1987a: An investigation of the El Niño–Southern Oscillation cycle with statistical models. 1. Predictor field characteristics. *J. Geophys. Res.*, **92** (C13), 14 251–14 270.

——, ——, and ——, 1987b: An investigation of the El Niño–Southern Oscillation cycle with statistical models. 2. Model results. *J. Geophys. Res.*, **92** (C13), 14 271–14 289.

Hasselmann, K., 1988: PIPs and POPs: The reduction of complex dynamical systems using Principal Interaction and Oscillation Patterns. *J. Geophys. Res.*, **93** (D9), 11 015–11 021.

Hotelling, H., 1935: Relations between two sets of variates. *Biometrica*, **28**, 321–377.

Inoue, M. and J. J. O'Brien, 1984: A forecasting model for the onset of El Niño. *Mon. Wea. Rev.*, **112**, 2326–2337.

Latif, M., 1987: Tropical ocean circulation experiments. *J. Phys. Oceanogr.*, **17**, 246–263.

——, and M. Flügel, 1991: An investigation of short range climate predictability in the tropical Pacific. *J. Geophys. Res.*, **96** (C2), 2661–2673.

——, A. Sterl, E. Maier-Reimer, and M. M. Junge, 1991: Interannual variability in a coupled GCM. Part 1: The tropical Pacific. *J. Climate,* **5,** (1992), in press.

Legler, D. M., and J. J. O'Brien, 1984: Atlas of tropical Pacific wind stress climatology 1971–1980. Florida State University, Department of Meteorology, Tallahassee, Florida, 182 pp.

Livezey, R. E., and W. Y. Chen, 1983: Statistical field significance and its determination by Monte Carlo techniques. *Mon. Wea. Rev.,* **111,** 46–59.

Neelin, J. D., 1991: The slow sea surface temperature mode and the fast-wave limit: Analytic theory for tropical interannual oscillations and experiments in a hybrid coupled model. *J. Atmos. Sci.,* **48,** 584–606.

Pacanowski, R. C., and S. G. H. Philander, 1981: Parameterization of vertical mixing in numerical models of tropical oceans. *J. Phys. Oceanogr.,* **11,** 1443–1451.

Pazan, S. E., W. B. White, M. Inoue, and J. J. O'Brien, 1986: Off-equatorial influence upon Pacific equatorial dynamic height variability during the 1982–1983 El Niño/Southern Oscillation event. *J. Geophys. Res.,* **91,** 8437–8449.

Philander, S. G. H., 1990: A review of simulations of the Southern Oscillation. *Proc. of the Int. TOGA Conference,* Honolulu, WMO/TD, No. 379.

——, and A. D. Seigel, 1985: Simulation of El Niño of 1982–1983. *Coupled Ocean–Atmosphere Models.* J. C. J. Nihoul, Ed., Elsevier Oceanography Series, No. 40.

Philander, S. G. H., R. C. Pacanowski, N. C. Lau, and M. J. Nath, 1991: A simulation of the Southern Oscillation with a global atmospheric GCM coupled to a high-resolution, tropical Pacific ocean GCM. *J. Climate,* **5,** (1992), in press.

Sausen, R., K. Barthel, and K. Hasselmann, 1988: Coupled ocean–atmosphere models with flux correction. *Climate Dyn.,* 145–163.

Schopf, P. S., and M. J. Suarez, 1988: Vacillations in a coupled ocean–atmosphere model. *J. Atmos. Sci.,* **45,** 549–566.

Storch, H. V., T. Bruns, I. Fischer-Bruns, and K. Hasselmann, 1988: Principal Oscillation analysis of the 30 to 60 day oscillation in a GCM. *J. Geophys. Res.,* **93** (D9), 11 022–11 036.

White, W. B., S. E. Pazan, and M. Inoue, 1987: Hindcast/forecast of ENSO events based upon the redistribution of observed and model heat content in the western tropical Pacific, 1964–86. *J. Phys. Oceanogr.,* **17,** 264–280.

Wyrtki, K., 1985: Water displacements in the Pacific and the genesis of El Niño cycles. *J. Geophys. Res.,* **90** (C4), 7129–7132.

Xu, J.-S., and H. V. Storch, 1990: Principal oscillation patterns—prediction of the state of ENSO. *J. Climate,* **3,** 1316–1329.

Zebiak, S. E., and M. A. Cane, 1987: A model El Niño–Southern Oscillation. *Mon. Wea. Rev.,* **115,** 2262–2278.